

Phase Equilibria Study of {*N*-Hexylisoquinolinium bis{(trifluoromethyl)sulfonyl}imide + Aromatic Hydrocarbons or an Alcohol} Binary Systems

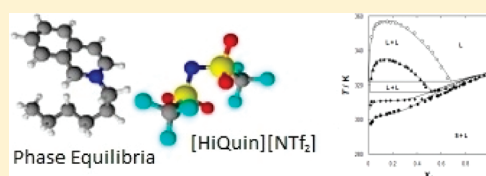
Urszula Domańska,^{*,†,‡} Maciej Zawadzki,[†] M. Marc Tshibangu,^{†,‡} Deresh Ramjugernath,[‡] and Trevor M. Letcher[‡]

[†]Department of Physical Chemistry, Faculty of Chemistry, Warsaw University of Technology, Noakowskiego 3, 00-664 Warsaw, Poland

[‡]Thermodynamic Research Unit, School of Chemical Engineering, University of KwaZulu-Natal, Howard College Campus, King George V Avenue, Durban 4001, South Africa

S Supporting Information

ABSTRACT: Isoquinolinium ionic liquid (IL) has been synthesized from *N*-hexylisoquinolinium bromide as a substrate. Specific basic characterization of the synthesized compound is included, which includes NMR spectra, elementary analysis, and water content. The basic thermal properties of the pure IL, that is, melting and solid–solid transition temperatures, as well as the enthalpy of fusion, or solid–solid transition have been measured using a differential scanning microcalorimetry technique. The density and viscosity as a function of temperature have been measured for the pure IL at temperatures higher than the melting temperature and were extrapolated to $T = 298.15$ K. The temperature–composition phase diagrams of 8 binary mixtures composed of the IL *N*-hexylisoquinolinium bis{(trifluoromethyl)sulfonyl}imide, ([HiQuin][NTf₂]) and an aromatic hydrocarbon (benzene, or toluene, or ethylbenzene, *n*-propylbenzene) or an alcohol (1-butanol, or 1-hexanol, or 1-octanol, or 1-decanol) have been determined from ambient temperature to the boiling-point temperature of the solvent at ambient pressure. A dynamic method was used over a broad range of mole fractions and temperatures from 270 to 330 K. For the binary systems, the eutectic diagrams were observed with immiscibility in the liquid phase with an upper critical solution temperature (UCST). In the case of the mixture {IL + benzene, or alkylbenzene} the eutectic systems with mutual immiscibility in the liquid phase with very high UCSTs were observed. These points were not detectable with our method and were observed at low IL mole fraction. For mixtures with alcohols, it was observed that with an increasing chain length of an alcohol, the solubility decreases and the UCST increases. The coexistence curves corresponding to liquid–liquid phase equilibrium boundaries and the solid–liquid phase equilibrium has been correlated using the well-known nonrandom two-liquid (NRTL) model.



INTRODUCTION

For mixtures for which conventional distillation is difficult to use, such as separation of olefins, aromatic hydrocarbons from aliphatic hydrocarbons, or sulfur compounds from aliphatic hydrocarbons, there is a need for special entrainers and special treatments in the field of hydrocarbon processing. Since the boiling points of these mixtures lie within narrow temperature ranges, new substances as ionic liquids (ILs) are under intensive investigation, to determine their potential as replacement solvents. ILs show an extremely low solubility in aliphatic hydrocarbons (e.g., *n*-hexane, *n*-heptane, *n*-decane) and the solubility decreases when the carbon chain length of the aliphatic hydrocarbon increases.^{1–3} Thus the success of the separation comes from having high solubility of aromatic hydrocarbons, including thiophene, in the ILs. The specific properties of ILs, that is, high selectivity in the separation of aromatic hydrocarbons, thiophene from aliphatic hydrocarbons, or separation of ethanol from the azeotropic mixture with *n*-heptane, makes ILs interesting for new technologies.^{4–9}

The first screening process to determine the possible use of an IL in extraction for separation processes is by the measurements of activity coefficients at infinite dilution.¹⁰ Recently we presented the activity coefficients at infinite dilution for *N*-octylisoquinolinium bis{(trifluoromethyl)sulfonyl}imide, [C₈iQuin][NTf₂].¹¹ The selectivity S_{12}^{∞} for the separation of thiophene and aliphatic hydrocarbons was 10.96 at $T = 328.15$ K. This new liquid at room temperature IL with an *n*-octyl substituent showed definite lower selectivities at infinite dilution than other ionic liquids with the bis{(trifluoromethyl)sulfonyl}imide anion and different cations such as pyridinium, pyrrolidinium, piperidinium, sulphonium, or phosphonium.^{12–16} Despite the larger capacity of [C₈iQuin][NTf₂] compared to bis{(trifluoromethyl)sulfonyl}imide-based ILs, we have assumed that it is possible

Received: January 4, 2011

Revised: March 1, 2011

Published: March 21, 2011

to improve the selectivity by decreasing the alkyl chain length in the cation of the IL. The increased charge screening and hydrophobic contribution from longer alkyl chains in the cation results in increased interaction with the *n*-alkane solvents and less interaction with aromatic hydrocarbon. Thus the next IL chosen by us is *N*-hexylisoquinolinium bis{(trifluoromethyl)sulfonyl}imide, [HiQuin][NTf₂], which is solid at room temperature but will probably improve the selectivity.

Knowledge of the phase equilibria, as (solid + liquid), (SLE) and (liquid + liquid), (LLE) is fundamental for the ILs to be effectively used as replacement solvents in extractive distillation or liquid–liquid extraction.^{17–20} Recently, a large number of experimental phase equilibrium data including the ILs quinolinium-based (*N*-butylquinolinium bis{(trifluoromethyl)sulfonyl}imide, [BQuin][NTf₂], and *N*-hexylquinolinium bis{(trifluoromethyl)sulfonyl}imide, [HQuin][NTf₂]) were measured in binary systems.^{21,22} In the systems with aromatic hydrocarbons, all binary mixtures show LLE with upper critical solution temperatures.^{21,22} The solubility of quinolinium-based ILs in alcohols has a slight dependence on the cation of the IL; [BQuin][NTf₂] and [HQuin][NTf₂] systems show eutectic mixtures with complete miscibility in the liquid phase for low chain length alcohols and eutectic mixtures with immiscibility gap in the liquid phase for 1-hexanol and longer chain alcohols.^{21,22}

Until recently, the most important and popular ILs considered as extractive solvents, imidazolium, pyridinium and pyrrolidinium-based ionic liquids with anions like bis{(trifluoromethyl)sulfonyl}imide anion [NTf₂][−], trifluoromethanesulfonate anion [CF₃SO₃][−], or thiocyanate anion [SCN][−], have attracted interest in different laboratories.^{2,23} The quinolinium-based ionic liquids were chosen as entrainers due to their great extraction potential in the desulfurization of oils (extraction of dibenzothiophene from *n*-dodecane)²⁴ and in the 1-hexene/*n*-hexane separation problem.²⁵ Thus the ILs based on quinolinium, or isoquinolinium cations are considered promising substances in terms of possible industrial application.

The goal of this work is to assess the suitability of [HiQuin][NTf₂] for use in solvent-enhanced separation processes. This paper is a continuation of our wide ranging investigation into phase equilibria for ILs' containing systems. The SLE and LLE data of new isoquinolinium-based IL ([HiQuin][NTf₂]) in binary systems with aromatic hydrocarbons and alcohols will be discussed as an extractive media in different separating processes. The data obtained are analyzed to determine the influence of the nature of the cation in comparison with other ionic liquids. Herein, the densities were measured and the molar volume of the hypothetical subcooled ionic liquid at 298.15 K was calculated. To gain important insights on how the molecules interact or how they behave in solution, the molecular interpretation of the solubility is discussed in the final part of this work.

EXPERIMENTAL PROCEDURES

Materials. The ionic liquid *N*-hexylisoquinolinium bis{(trifluoromethyl)sulfonyl}imide, [HiQuin][NTf₂] used in this work was synthesized in our laboratory from *N*-hexylisoquinolinium bromide [HiQuin][Br].

For the synthesis of [HiQuin][Br], a 500 cm³ flask in an oil bath, equipped with a magnetic stirrer, condenser, and drying tube, was used. To a solution of 100 g of isoquinoline (distilled, Aldrich 97%), (0.6953 mol) in 200 cm³ of acetonitrile, 157.53 g of hexylbromide (as received, Aldrich 99%) (0.9543 mol, 1.23 equivalents) were added. The stirred mixture was heated and refluxed for 24 h. Afterward 100 cm³ of hexane was added, and a second phase formed. Acetonitrile was added until the mixture became a single phase. The mixture was left to cool overnight in the refrigerator. The white powder was filtrated and washed with hexane. The solvent was removed under vacuum and the product dried under vacuum at 353.15 K for 12 h. The yield was 197.30 g (86.6% of the theoretical value). The following information was determined for our sample.

¹H NMR (400 MHz, CDCl₃): δ = 0.744 (t, 3H, *J* = 6.802), 1.205 (m, 4H), 1.354 (m, 2H), 2.081 (pent, 2H, *J* = 7.602), 5.033 (t, 2H), 7.867 (m, 1H), 8.054 (m, 1H), 8.128 (d, 1H, *J* = 4.001), 8.408 (d, 1H, *J* = 6.402), 8.716 (d, 1H, *J* = 8.402), 8.900 (d, 1H, *J* = 6.802).

¹³C NMR (100 MHz, CDCl₃): δ = 13.739, 22.149, 25.592, 30.976, 31.697, 61.325, 126.262, 126.967, 127.695, 131.032, 131.054, 134.497, 136.841, 137.144, 150.119.

For the synthesis of [HiQuin][NTf₂], a 750 cm³ flask was used. A sample of 53.99 g of lithium bis{(trifluoromethyl)sulfonyl}imide (as received, Aldrich 99%) (0.1881 mol, 1.16 equivalents) was added to a solution of 47.60 g of [HiQuin][Br] (synthesized) (0.1618 mol) in 500 cm³ water. The solution became lighter in color and a second heavier phase formed. The mixture was stirred for 24 h, and afterward the phases were separated. The heavier phase was diluted with 50 cm³ of dichloromethane and extracted with distilled water until aqueous phase gave negative response on addition of AgNO₃. Dichloromethane was removed under vacuum, and the product was dried under vacuum at 353.15 K for 12 h. The yield was 74.12 g (92.6% of theoretical value). The following information was determined for our sample.

¹H NMR (400 MHz, CDCl₃): δ = 0.848 (t, 3H, *J* = 7.2), 1.335 (m, 6H), 2.066 (quint, 2H, *J* = 7.6), 4.728 (t, 2H, *J* = 7.6), 7.990 (m, 1H), 8.157 (m, 2H), 8.336 (d, 1H, *J* = 6.8), 8.471 (m, 2H), 9.709 (s, 1H).

¹³C NMR (400 MHz, CDCl₃): δ = 13.723, 22.210, 25.615, 30.923, 31.530, 62.190, 115.054, 118.246, 121.446, 124.639, 126.808, 127.195, 127.923, 130.819, 131.729, 134.012, 148.969.

The elementary microanalysis. Found: C, 41.26%; N, 5.86%; H, 3.94%; S, 14.80%. Theory: C, 41.29%; N, 5.67%; H, 4.08%; S, 12.97%.

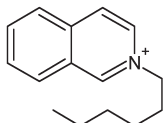
The NMR spectra for these two compounds are shown as GRS 1 to 4 in the Supporting Information.

The IL was further purified by subjecting the liquid to a very low pressure of about 5×10^{-3} Pa at a temperature about 280 K for approximately 5 h. This procedure removed any volatile chemicals and water from the ionic liquid. The structure of the investigated ionic liquid and the different physicochemical properties are listed in Table 1.

The purity in mass fraction and supplier of each of the aromatic compounds were as follows: benzene (CAS No. 71-43-2, Sigma-Aldrich, >99.97%); toluene (CAS No. 108-88-3, Fluka, >99.7%); ethylbenzene (CAS No. 100-41-4, Sigma-Aldrich, 99%); *n*-propylbenzene (CAS No. 103-65-1, Sigma-Aldrich, 98%).

The alcohols used in phase equilibria measurements were purchased from Sigma Aldrich Chemie GmbH (Steinheim,

Table 1. Investigated IL: Chemical Structure, Name, Abbreviation, and Measured Thermophysical Properties^a

structure	name				
	N-hexylisoquinolinium bis((trifluoromethyl)sulfonyl)imide				
	Abbreviation				
	[HiQuin][NTf ₂]	M	$V_{m,1}(298.15)$		
		(g·mol ⁻¹)	(cm ³ ·mol ⁻¹)		
		494.47	358.53		
	$T_{fus,1}$	$\Delta_{fus}H_1$	$T_{tr,1}$	$\Delta_{tr}H_1$	
	(K)	(kJ·mol ⁻¹)	(K)	(kJ·mol ⁻¹)	
	327.2	58.64	193.8	2.45	

^a Molar volume ($V_{m,1}$) at $T = 298.15$ K, temperature and enthalpy of fusion ($T_{fus,1}$ and $\Delta_{fus}H_1$, respectively), phase transition temperature ($T_{tr,1}$), and enthalpy change at $T_{tr,1}$ ($\Delta_{tr}H_1$).

Table 2. Density and Viscosity (Dynamic and Kinematic) for [HiQuin][NTf₂]

T/K	$\eta_{dyn}/\text{mPa}\cdot\text{s}$	$\eta_{kin}/\text{mm}^2\cdot\text{s}^{-1}$	$\rho/\text{g}\cdot\text{cm}^{-3}$
328.2	64.807	47.881	1.35350
333.2	52.353	38.803	1.34919
338.2	42.918	31.912	1.34489
343.2	35.569	26.532	1.34060
348.2	29.865	22.349	1.33632
353.2	25.379	19.052	1.33206
358.2	21.841	16.449	1.32778
363.2	18.711	14.137	1.32353
298.2	160.91 ^a	117.92 ^a	1.37915 ^a

^a Extrapolated values: density, $\rho/\text{g}\cdot\text{cm}^{-3} = -8.562 \times 10^{-4}(T/K)^3 + 1.63443$; dynamic viscosity, $\eta_{dyn}/\text{mPa}\cdot\text{s} = 0.03018(T/K)^2 - 22.1343(T/K) + 4077.379$; kinematic viscosity, $\eta_{kin}/\text{mm}^2\cdot\text{s}^{-1} = 0.02192(T/K)^2 - 16.0868(T/K) + 2965.240$.

Germany). All the alcohols were fractionally distilled to achieve a mass percent purity (checked by using gas chromatography) of >99.8% and then stored over freshly activated molecular sieve (type 4A from Union Carbide).

Differential Scanning Microcalorimetry (DSC). The temperature of fusion ($T_{fus,1} = 326.5$ K), enthalpy of fusion ($\Delta_{fus}H_1 = 58.64$ kJ·mol⁻¹), the solid–solid phase transition temperature ($T_{tr,1} = 193.8$ K), and the phase transition enthalpy ($\Delta_{tr}H_1 = 2.45$ kJ·mol⁻¹) have been measured using a differential scanning microcalorimetry technique (DSC). The applied scan rate was 5 K·min⁻¹ with a power and recorder sensitivity of 16 mJ·s⁻¹ and 5 mV, respectively. The apparatus (Thermal Analysis Q200, U.S.A. with liquid nitrogen cooling system) was calibrated with a 0.999999 mol fraction purity indium sample. The average value of the melting temperature was ($T_{fus,1} \pm 0.1$) K (average over three scans). The repeatability of that value was ± 0.1 K. The enthalpy of fusion was ($\Delta_{fus}H_1 \pm 0.1$) kJ·mol⁻¹. The thermophysical properties are shown in Table 1 and GRS S5 in the Supporting Information. The melting temperature observed during the solubility measurements was slightly higher, $T_{fus,1} = 327.2$ K.

Water Content. The water content was analyzed by the Karl Fischer titration technique (method TitroLine KF). The sample of IL was dissolved in methanol and titrated with steps of 2.5 μL . The results obtained have shown the water content to be less than 310 ppm. The error on the water content was ± 10 ppm for the 3 mL of injected IL.

Density Measurements. The density of the IL was measured using an Anton Paar GmbH 4500 vibrating-tube densimeter

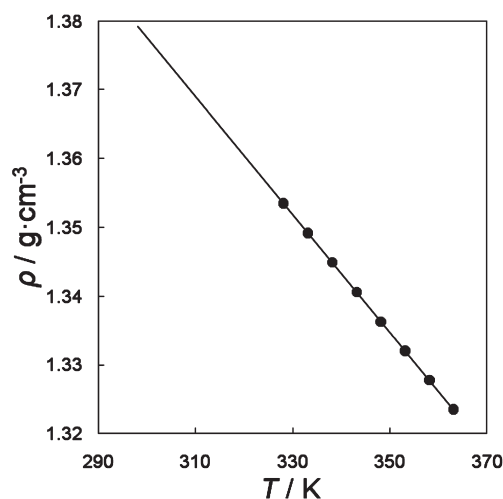


Figure 1. Plot of the density as a function of temperature for [HiQuin][NTf₂]. Solid lines represent the linear approximation.

(Graz, Austria), thermostatted at different temperatures. Two integrated Pt 100 platinum thermometers provided good precision in temperature control internally ($T \pm 0.01$ K). Densimeter includes an automatic correction for the viscosity of the sample. The calibration for temperature and pressure was made by the producer. The apparatus is precise to within 1×10^{-5} g·cm⁻³, and the uncertainty of the measurements was estimated to be better than $\pm 1 \times 10^{-4}$ g·cm⁻³. The densimeter's calibration was performed at atmospheric pressure using doubly distilled and degassed water, specially purified benzene (CHEMIPAN, Poland 0.999), and dried air. The densities of the IL over a temperature range (328 to 363) K are shown in Table 2 and in Figure 1).

Viscosity Measurements. Viscosity measurements were carried out in an Anton Paar BmbH AMVn (Graz, Austria) programmable rheometer, with a nominal uncertainty of $\pm 0.1\%$ and reproducibility <0.05% for viscosities from 0.3 to 2500 mPa·s. Temperature was controlled internally with a precision of ± 0.01 K in a range from 328.2 to 363.2 K. The diameter of the capillary was 3.0 mm for viscosities from 2.5 to 70 mPa·s and the diameter of the ball was 2.0 mm for the higher viscosities. The error for this capillary was <0.01%. The dynamic and kinematic viscosities are listed in Table 2 and are shown in Figure 2.

Solid–Liquid and Liquid–Liquid Phase Equilibria Apparatus and Measurements. Solid solubilities or the disappearance of two phases observed with an increasing temperature have

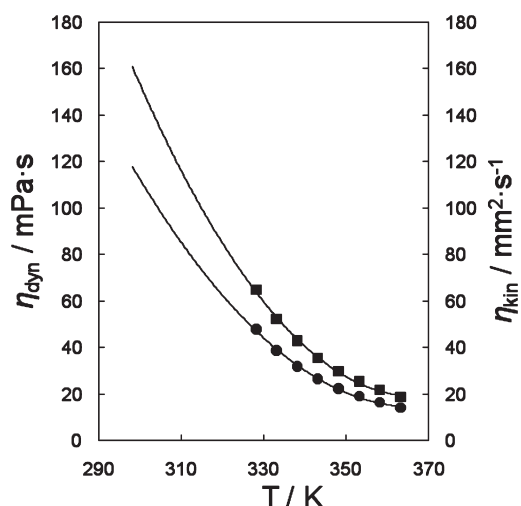


Figure 2. Plot of the viscosity temperature dependence of [HiQuin][NTf₂]. Solid lines represent polynomial approximation. Points are the experimental results: ●, kinematic viscosity, ■, dynamic viscosity.

been determined using a dynamic (synthetic) method described previously.^{3,11–13} The compound was kept under nitrogen in a dry box. Mixtures of solute and solvent were prepared by weighing the pure components to within 1×10^{-4} g. The sample of solute and solvent was heated very slowly (at less than $2 \text{ K} \cdot \text{h}^{-1}$ near the equilibrium temperature) with continuous stirring inside a Pyrex glass cell placed in a thermostat. The thermostat was filled up with water or acetone with dry ice. The next experimental point was made after the weighing the vessel and adding the solvent changing the mole fraction of the sample. The apparatus is presented as Figure 1S in the Supporting Information. The crystal disappearance temperatures, or foggy solution disappearance detected visually, were measured with a calibrated Gallenkamp Auto-therm II thermometer. The measurements were carried out over a wide range of solute mole fractions ranging from 0 to 1. The uncertainty of temperature measurements was $\pm 0.05 \text{ K}$ and that of the mole fraction did not exceed ± 0.0005 . The reproducibility of the SLE and LLE experimental points was $\pm 0.1 \text{ K}$. The experimental results are listed in Tables 3–5.

RESULTS AND DISCUSSION

The basic thermal properties of the ionic liquid [HiQuin][NTf₂] (the enthalpy of fusion and the melting temperature) show a big difference between this IL and that observed for [C₈iQuin][NTf₂], which was liquid at room temperature.¹¹ The comparison with [HQuin][NTf₂]²² shows that [HiQuin][NTf₂] has lower density, lower viscosity, and surprisingly higher melting temperature and lower enthalpy of melting than [HQuin][NTf₂]. The molecule of [HQuin][NTf₂] is more compact and reveals stronger interaction between the anion and cation.

This work focuses on the difference between the solvent quality toward the selected IL, [HiQuin][NTf₂], in comparison with [HQuin][NTf₂] and [BQuin][NTf₂], which differ slightly on the nature of their constituting cations ([HiQuin]⁺ versus [HQuin]⁺ or [BQuin]⁺).

The experimental data (temperature vs mole fraction of the IL) for the binary systems with benzene, alkylbenzenes, and

Table 3. SLE of the Binary Systems {[HiQuin][NTf₂] (1) + Aromatic Hydrocarbon (2)} (γ_1 , the Activity Coefficient at Saturated Solution)

x_1	T^{SLE}/K	γ_1	x_1	T^{SLE}/K	γ_1
Benzene					
1.0000	327.2 ^a	1.00	0.2793	278.6 ^a	0.08
0.9544	326.4 ^a	0.99	0.2403	271.3 ^a	0.05
0.8952	325.0 ^a	0.97	0.2158	270.1 ^a	0.05
0.8186	322.1 ^a	0.87	0.1932	272.8 ^b	1.13
0.7450	319.5 ^a	0.80	0.1809	274.1 ^b	1.14
0.6923	317.4 ^a	0.74	0.1707	275.0 ^b	1.14
0.6334	313.9 ^a	0.63	0.1572	276.0 ^b	1.14
0.5882	311.2 ^a	0.56	0.1440	276.9 ^b	1.14
0.5393	307.9 ^a	0.48	0.1323	277.7 ^b	1.14
0.4737	302.5 ^a	0.36	0.1213	278.2 ^b	1.13
0.4237	298.4 ^a	0.29	0.1151	278.4 ^b	1.13
0.3780	293.4 ^a	0.22	0.1093	278.6 ^b	1.12
0.3287	286.5 ^a	0.14	0.1041	278.6 ^b	1.12
Toluene					
1.0000	327.2	1.00	0.4578	301.0	0.33
0.9606	326.0	0.96	0.4181	297.2	0.27
0.9080	324.6	0.93	0.3684	291.4	0.19
0.8589	322.9	0.88	0.3124	285.3	0.14
0.8092	321.3	0.83	0.2626	278.9	0.09
0.7562	319.1	0.76	0.2141	271.2	0.05
0.6967	316.4	0.69	0.1819	267.2	0.04
0.6097	312.3	0.59	0.1549	262.5	0.03
0.5575	308.9	0.50	0.1306	256.7	0.02
0.5012	304.8	0.41	0.1052	256.7	0.03
Ethylbenzene					
1.0000	327.2	1.00	0.4784	305.3	0.45
0.9379	325.4	0.95	0.4299	302.1	0.39
0.8830	323.6	0.89	0.3667	297.5	0.32
0.7946	320.6	0.81	0.3240	294.1	0.27
0.7152	317.3	0.72	0.2802	289.9	0.22
0.6424	314.3	0.64	0.2364	286.0	0.19
0.5744	310.8	0.56	0.2038	283.4	0.18
0.5299	308.6	0.51	0.1746	282.0	0.18
<i>n</i> -Propylbenzene					
1.0000	327.2	1.00	0.4368	305.0	0.48
0.9321	325.7	0.97	0.3870	302.2	0.44
0.8602	323.7	0.92	0.3473	299.9	0.40
0.8224	322.3	0.88	0.3126	297.6	0.37
0.7420	319.5	0.80	0.2876	296.5	0.37
0.6762	316.8	0.73	0.2677	295.4	0.37
0.6204	314.4	0.67	0.2620	294.8	0.36
0.5547	311.2	0.60	0.2470	294.2	0.36
0.4832	307.5	0.52	0.2293	294.0	0.38

^a IL liquidus curve. ^b Solvent liquidus curve.

alcohols are presented in Figures 3–5, respectively. The phase diagrams for {[HiQuin][NTf₂] + aromatic hydrocarbon} depicting liquid–liquid immiscibility windows at low mole fraction of the IL. The solubility of aromatic hydrocarbons in the IL is high and the immiscibility gap started from mole fraction

Table 4. SLE of the Binary Systems {[HiQuin][NTf₂] (1) + 1-Butanol or 1-Hexanol (2)} (γ_1 , the Activity Coefficient at Saturated Solution)

x_1	T^{SLE}/K	γ_1	x_1	T^{SLE}/K	γ_1
1-Butanol					
1.0000	327.2	1.00	0.4072	308.9	0.68
0.9712	326.0	0.95	0.3493	307.6	0.72
0.8957	324.0	0.90	0.2495	305.3	0.86
0.8426	322.3	0.85	0.2108	304.7	0.96
0.7807	320.4	0.81	0.1753	303.9	1.09
0.7229	318.6	0.77	0.1514	303.2	1.20
0.6725	317.1	0.75	0.0995	302.5	1.73
0.6307	315.6	0.72	0.0636	301.5	2.50
0.5740	313.9	0.70	0.0330	299.0	3.95
0.5129	312.0	0.68	0.0185	297.7	6.36
0.4673	310.6	0.68			
1-Hexanol					
1.0000	327.2	1.00	0.4981	312.6	0.73
0.9476	325.4	0.94	0.4403	311.9	0.79
0.8812	323.5	0.89	0.3829	311.7	0.89
0.8276	322.1	0.86	0.3378	311.5	1.00
0.7932	320.7	0.81	0.2973	311.2	1.11
0.7482	319.3	0.78	0.2427	311.0	1.34
0.7088	318.4	0.78	0.1802	310.9	1.79
0.6846	317.6	0.76	0.1444	310.8	2.22
0.6505	316.1	0.72	0.0983	310.6	3.21
0.5952	314.4	0.70	0.0432	310.4	7.21
0.5633	313.7	0.70	0.0224	310.3	13.80
0.5223	313.2	0.73	0.0146	308.4	18.41

$x_1 = 0.1$ for benzene and $x_1 = 0.2$ for *n*-propylbenzene (see Figures 3 and 4). The eutectic point for [HiQuin][NTf₂] (1) + benzene (2) is $x_{1,e} = 0.193 \pm 0.002$, $T_e/\text{K} = 272.8 \pm 0.5$.

For the other mixtures with aromatic solvents, the eutectic point is shifted to the very low mole fraction of the solvent, because the melting temperatures of the toluene (178.15 K), ethylbenzene (179.15 K), and *n*-propylbenzene (173.15 K) are much lower than those for benzene (278.65 K). Thus the phase diagrams of these three systems are different than this for {IL + benzene}. The interaction of the IL and aromatic solvents is quite high, because the solubility of the IL in benzene, and alkylbenzenes is higher than the ideal solubility (see dotted lines in Figures 3 and 4). The solubility of organic compounds in the [HiQuin][NTf₂] is higher than in [HQuin][NTf₂].²² We assume that the solubility in the aliphatic hydrocarbons is similar. The comparison of phase diagrams for the binary systems of {IL (1) + aromatic hydrocarbon (2)} for ILs with the same anion [NTf₂][−] but different quinolinium cations, [HiQuin]⁺ and [BQuin]⁺, shows the lowest solubility of aromatic hydrocarbons in [BQuin][NTf₂].²¹ It can be observed from the hierarchy that increasing the length of the alkyl chain flanking the quinolinium cation for a fixed anion, that is, [NTf₂][−] is favorable for increasing the melting point, thus decreasing the solubility. Analyzing the possible use of [HiQuin][NTf₂] for the separation of the aliphatics from aromatics the discussion of the solubility of *n*-alkanes and benzene, or alkylbenzenes in the IL has to be compared for different ILs. From the obtained results the

Table 5. SLE and LLE of the Binary Systems {[HiQuin][NTf₂] (1) + 1-Octanol or 1-Decanol (2)}

x_1	T^{SLE}/K	T^{LLE}/K	x_1	T^{SLE}/K	T^{LLE}/K
1-Octanol					
1.0000	327.2		0.3880	316.4	326.5
0.9612	326.3		0.3538	316.4	328.6
0.9152	325.0		0.3256	316.4	330.3
0.8793	323.9		0.3055	316.4	331.0
0.7931	321.7		0.2572	316.4	332.6
0.7824	321.2		0.2205	316.4	333.8
0.7653	321.0		0.1997	316.4	334.3
0.7016	319.3		0.1730	316.4	334.7
0.6382	318.3		0.1273	316.4	334.8
0.5843	317.5		0.0975	316.4	334.6
0.5738	317.3		0.0653	316.4	333.5
0.5462	317.0		0.0616	316.4	332.8
0.5190	316.7		0.0470	316.4	331.5
0.4725	316.4	319.1	0.0365	316.4	329.0
0.4594	316.4	321.0	0.0330	316.4	328.8
0.4288	316.4	323.4	0.0212	316.4	324.0
1-Decanol					
1.0000	327.2		0.4440	320.6	345.6
0.9743	326.3		0.3788	320.6	350.1
0.9357	325.6		0.3208	320.6	353.0
0.8939	324.4		0.2693	320.6	354.9
0.8608	323.4		0.2257	320.6	356.0
0.8224	322.7		0.1827	320.6	356.6
0.7652	321.4		0.1528	320.6	356.8
0.7156	320.7		0.1155	320.6	356.6
0.6538	320.6	324.2	0.0910	320.6	356.3
0.6026	320.6	330.5	0.0684	320.6	355.5
0.5658	320.6	334.9	0.0547	320.6	354.3
0.5296	320.6	339.0	0.0421	320.6	352.7
0.4919	320.6	341.9	0.0265	320.6	348.0

[HiQuin][NTf₂] is the most promising in comparison with [HQuin][NTf₂] and [BQuin][NTf₂].

The interaction of the IL with aromatic hydrocarbons coming from the availability of localized or delocalized π -electron clouds, lone pair electrons, and permanent dipoles enhances the affinity of the IL for organic solvents.

On the basis of the phase diagrams with an alcohol, the following trends can be observed: for all systems, the eutectic mixtures with miscibility gap for the longer chains alcohols was observed; the solubility of the IL in alcohols decreases as the length of carbon chain of an alcohol increases; the eutectic temperatures are expected far below 260 K and at very low mole fraction of the IL. In general the solubility of [HiQuin][NTf₂] in alcohols is higher than those of [HQuin][NTf₂] for which the complete miscibility in the liquid phase was observed up to 1-butanol,²² whereas [HiQuin][NTf₂] shows immiscibility in the liquid phase for 1-octanol and for the longer chains alcohols.

The experimental phase diagrams with alcohols are shown in Figure 5. The upper critical solution temperature (UCST) of the miscibility gap is lower for the [HiQuin][NTf₂] in comparison with [HQuin][NTf₂] and [BQuin][NTf₂].^{21,22}

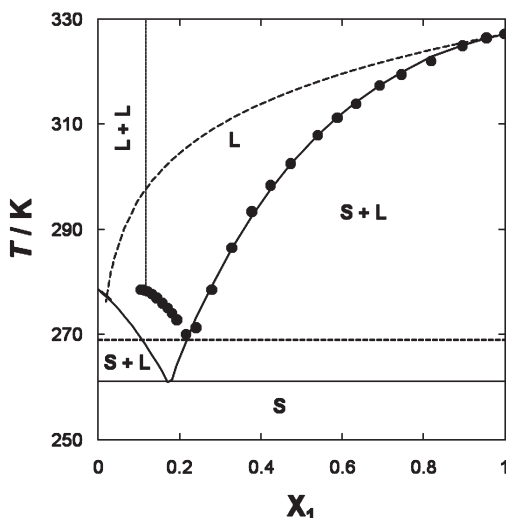


Figure 3. Plot of the experimental and calculated SLE of {[HiQuin][NTf₂]}(1) + benzene (2) system. The dotted line represents the ideal solubility. Solid lines have been calculated using the nonrandom two-liquid NRTL equation.

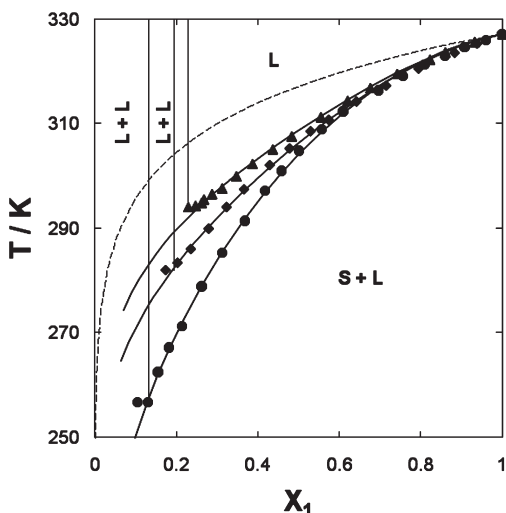


Figure 4. Plot of the experimental and calculated SLE of {[HiQuin][NTf₂]}(1) + aromatic hydrocarbon (2) binary systems: ●, toluene; ◆, ethylbenzene; ▲, *n*-propylbenzene. The dotted line represents the ideal solubility; solid lines have been calculated using the NRTL equation.

MODELING

(Solid–Liquid) Phase Equilibrium Correlation. Since the solid–solid phase transition was observed at a very low temperature, and the change of heat capacity at the melting temperature was not measured, a simplified general thermodynamic equation relating temperature, T^{SLE} and the mole fraction of the IL, x_1 in all solvents has been fitted with the same parameters obtained from the correlation of SLE experimental data according to the equation²⁶

$$-\ln x_1 = \frac{\Delta_{\text{fus}}H_1}{R} \left(\frac{1}{T^{\text{SLE}}} - \frac{1}{T_{\text{fus},1}} \right) + \ln \gamma_1 \quad (1)$$

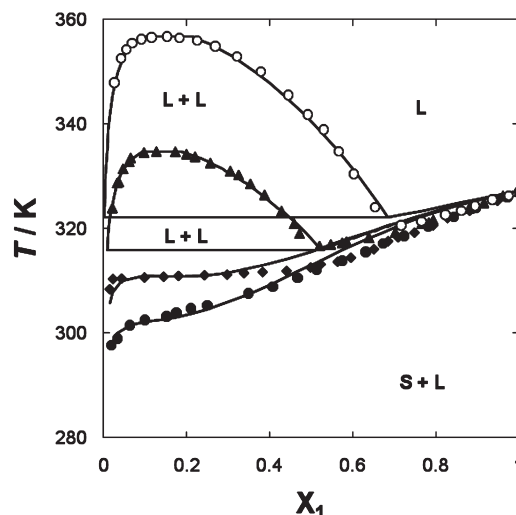


Figure 5. Plot of the experimental and calculated SLE of {[HiQuin][NTf₂]}(1) + an alcohol (2) binary systems: ●, 1-butanol; ◆, 1-hexanol; ▲, 1-octanol; ○, 1-decanol. The solid lines have been calculated using the NRTL equation. For the sake of clarity the SLE points in the region of immiscibility have not been presented in the figure.

Table 6. Correlation of the SLE Data by Means of the NRTL Equation, σ_T , the Temperature Deviation

solvent	NRTL ^a parameters		rmsd
	Δg_{12}	$\Delta g_{21}/(\text{J} \cdot \text{mol}^{-1})$	
benzene	−6844.1	−2308.52	0.74 ^b /12.3 ^c
toluene	−5067.7	−3606.9	0.57
ethylbenzene	−466.6	−5184.6	0.51
<i>n</i> -propylbenzene	−4871.7	−6832.9	0.36

^a $\alpha = 0.2$. ^b The IL liquidus curve. ^c Solvent liquidus curve.

where $T_{\text{fus},1}$, $\Delta_{\text{fus}}H_1$, T^{SLE} , x_1 , and γ_1 refer to melting temperature for the pure IL; enthalpy of fusion for the pure IL; (solid + liquid) equilibrium temperature; equilibrium mole fraction; and the activity coefficient of the IL in the saturated solution, respectively. The first two values are given in Table 1, and the experimental data are listed in Tables 2'–4. The enthalpy of melting is assumed to be temperature independent, whereas the activity coefficients are temperature, as well as solubility dependent.

In this study, the NRTL model²⁷ was used to correlate the SLE phase equilibria. The NRTL equation has two adjustable parameters P_1 and P_2 (the α parameter is fixed, additionally), which are determined by minimization of the objective function $F(P_1, P_2)$, defined as follows

$$F(P_1, P_2) = \sum_{i=1}^n [T_{\text{exp},i} - T_{\text{calc},i}(x_i, P_1, P_2)]^2 \quad (2)$$

where n denotes the number of experimental points. The Marquardt algorithm for solving nonlinear least-squares problems was successfully used in this work. As a measure of the reliability of the correlations, the root-mean-square deviation of temperature, σ_T , has been calculated according to the

Table 7. Correlation of the SLE and LLE Data by Means of the NRTL Equation, σ_x , the Composition Deviation; σ_T , the Temperature Deviation

solvent	NRTL parameters ^a				rmsd	
	$a_{12}/(\text{J} \cdot \text{mol}^{-1})^b$	$a_{21}/(\text{J} \cdot \text{mol}^{-1})$	$b_{12}/(\text{J} \cdot \text{mol}^{-1} \cdot \text{K}^{-1})^b$	$b_{21}/(\text{J} \cdot \text{mol}^{-1} \cdot \text{K}^{-1})$	σ_x	$\sigma_T/(\text{K})$
1-butanol	31855.6	−6717.7	−123.93	65.87		1.44
1-hexanol	29005.3	200.0	−107.45	41.50		2.52
1-octanol	29050.8	38819.0	−101.00	−74.52	0.0024	1.79
1-decanol	30503.8	35723.5	−98.81	−59.82	0.0047	1.59

^a $\alpha = 0.2$. ^b $(g_{12} - g_{22})/(\text{J} \cdot \text{mol}^{-1}) = (a_{12} + b_{12})(T/\text{K})$; $(g_{12} - g_{11})/(\text{J} \cdot \text{mol}^{-1}) = (a_{21} + b_{21})(T/\text{K})$.

following definition

$$\sigma_T = \left\{ \sum_{i=1}^n \frac{(T_{\text{exp},i} - T_{\text{calc},i})^2}{n-2} \right\}^{1/2} \quad (3)$$

The values of the NRTL parameters and the corresponding root-mean-square deviations of temperature, σ_T , are reported in Tables 6 and 7 and the resulting curves are presented together with the experimental points in Figures 3 to 5. The activity coefficients were computed from the values of SLE data to screen the deviations from the ideality. The values of the activity coefficients at saturated solutions were lower than one for aromatic hydrocarbons and higher than one for the alcohols close and under the immiscibility region.

The results obtained indicate that the equation used was appropriate in providing a reliable description of the SLE measured in this work. The average value of the root-mean-square deviations of temperature, σ_T , was 0.54 K for aromatic hydrocarbons for example and the IL liquidus curves.

(Liquid–Liquid) Phase Equilibrium Correlation. The adjustable parameters $(g_{12} - g_{22})$ and $(g_{21} - g_{11})$ of the model were found by minimizing the objective function (OF)

$$\text{OF} = \sum_{i=1}^n [(\Delta x_1)_i^2 + (\Delta x_1^*)_i^2] \quad (4)$$

where n is the number of experimental points, x is a mole fraction in the IL-rich phase, x^* is the IL-poor phase, and Δx is defined as

$$\Delta x = x_{\text{calc}} - x_{\text{exp}} \quad (5)$$

The root-mean-square deviation of the mole fraction was defined as

$$\sigma_x = \left(\sum_{i=1}^n \frac{(\Delta x_1)_i^2}{n-2} + \sum_{i=1}^n \frac{(\Delta x_1^*)_i^2}{n-2} \right)^{1/2} \quad (6)$$

In this calculation, the parameter α_{12} is a constant of proportionality similar to the nonrandomness constant of the NRTL equation ($\alpha_{12} = \alpha_{21} = 0.2$) and was taken into account by choosing the value that gave the lowest deviation. The calculated values of the NRTL parameters and the corresponding root-mean-square deviations for the alcohol systems are presented in Table 7. The average deviation is in the range $\sigma_x = 0.0035$.

CONCLUDING REMARKS

With this researching work and some our previous papers, the ability of isoquinolinium-based IL, [HiQuin][NTf₂], to extraction aromatic hydrocarbons from aliphatic hydrocarbons has been discussed. The high solubility of [HiQuin][NTf₂] in

benzene and low as usual in alkanes confirm the suitability of this IL as solvent-enhanced for separation processes.

Phase equilibrium data, including SLE and LLE, for binary mixtures of the ionic liquid [HiQuin][NTf₂] with benzene, alkylbenzenes, and 1-alcohols have been measured. The (solid + liquid) phase diagrams for all the systems studied here show an eutectic systems and immiscibility in the liquid phase with exception of 1-butanol and 1-hexanol binary systems. The results were compared to analogous ionic liquids with the same anion and similar quinolinium/isoquinolinium cation. A comparison of phase diagrams indicate that an exchange of the cation, [HQuin]⁺ for [HiQuin]⁺, changes the physicochemical properties and solubility of the IL in aromatic hydrocarbons and alcohols, decreasing the UCST. Benzene and alkylbenzenes showed a much higher solubility in [HiQuin][NTf₂] than alcohols.

The mathematical description of the SLE and LLE data was carried out by means of the NRTL equation. The results of the correlation were acceptable for all the data.

ASSOCIATED CONTENT

S Supporting Information. ¹H NMR spectra and ¹³C NMR spectra for [HiQuin]Br and [HiQuin][NTf₂]; DSC diagram for [HiQuin][NTf₂]; and figure of the apparatus for the solubility measurements. This material is available free of charge via the Internet at <http://pubs.acs.org>.

AUTHOR INFORMATION

Corresponding Author

*E-mail: ula@ch.pw.edu.pl. Fax: +48 22 6282741. Phone: +48 22 6213115.

ACKNOWLEDGMENT

Funding for this research was provided by the Polish Ministry of Education and Sciences for the Joint Project of Polish-South African Scientific and Technological International Cooperation.

REFERENCES

- (1) Domańska, U.; Królikowski, M.; Pobudkowska, A.; Letcher, T. M. *J. Chem. Eng. Data* **2009**, *54*, 1435–1441.
- (2) Domańska, U. *Ionic Liquids in Chemical Analysis*; CRC Press, Taylor & Francis Group: Abingdon, U.K., 2008; Chapter 1.
- (3) Domańska, U.; Marciniak, A. *Fluid Phase Equilib.* **2007**, *260*, 9–18.
- (4) Arce, A.; Earle, M.; Katdare, S.; Rodríguez, H.; Seddon, K. S. *Phys. Chem. Chem. Phys.* **2008**, *10*, 2358–2542.

- (5) Alonso, L.; Arce, A.; Francisco, M.; Soto, A. *J. Chem. Eng. Data* **2010**, *55*, 3262–3267.
- (6) Seeberger, A.; Jess, A. *Green Chem.* **2010**, *12*, 602–608.
- (7) Zhang, J.; Zhu, W.; Li, H.; Jiang, W.; Huang, W.; Yan, Y. *Green Chem.* **2010**, *12*, 1801–1807.
- (8) Arce, A.; Earle, M.; Rodríguez, H.; Seddon, K. R.; Soto, A. *Green Chem.* **2009**, *11*, 365–372.
- (9) Kohler, F.; Roth, D.; Kuhlmann, E.; Wasserscheid, P.; Haumann, M. *Green Chem.* **2010**, *12*, 979–984.
- (10) Marciniak, A. *Fluid Phase Equilib.* **2010**, *294*, 213–233.
- (11) Domańska, U.; Zawadzki, M.; Królikowska, M.; Tshibangu, M. M.; Ramjugernath, D.; Letcher, T. M. *J. Chem. Thermodyn.* **2011**, *43*, 499–504.
- (12) Domańska, U.; Marciniak, A. *Fluid Phase Equilib.* **2009**, *286*, 154–161.
- (13) Zhang, J.; Zhang, Q.; Qiao, B.; Deng, Y. *J. Chem. Eng. Data* **2007**, *52*, 2277–2283.
- (14) Domańska, U.; Marciniak, A. *J. Chem. Thermodyn.* **2009**, *41*, 1350–1355.
- (15) Domańska, U.; Marciniak, A. *J. Chem. Thermodyn.* **2009**, *41*, 754–758.
- (16) Domańska, U.; Paduszyński, K. *J. Chem. Thermodyn.* **2010**, *42*, 1361–1366.
- (17) Arce, A.; Francisco, M.; Soto, A. *J. Chem. Thermodyn.* **2010**, *42*, 712–717.
- (18) Domańska, U.; Królikowska, M.; Królikowski, M. *Fluid Phase Equilib.* **2010**, *294*, 72–83.
- (19) Domańska, U.; Laskowska, M.; Pobudkowska, A. *J. Phys. Chem B* **2009**, *113*, 6397–6404.
- (20) Deive, F. J.; Rodríguez, A.; Pereiro, A. B.; Shimizu, K.; Forte, P. A. S.; Romão, C. C.; Lopes, J. N. C.; Esperança, J. M. S. S.; Rebelo, L. P. N. *J. Phys. Chem B* **2010**, *114*, 7329–7337.
- (21) Domańska, U.; Zawadzki, M.; Tshibangu, M. M.; Ramjugernath, D.; Letcher, T. M. *J. Chem. Thermodyn.* **2010**, *42*, 1180–1186.
- (22) Domańska, U.; Zawadzki, M.; Zwolińska, M. *J. Chem. Thermodyn.* **2011**, *43*, 775–781.
- (23) Meindersma, G. W.; Hansmeier, A. R.; de Hann, A. B. *Ind. Eng. Chem. Res.* **2010**, *49*, 7530–7540.
- (24) Holbrey, J. D.; López-Martin, I.; Rothenberg, G.; Seddon, K. S.; Silvero, G.; Zheng, X. *Green Chem.* **2008**, *10*, 87–92.
- (25) Lei, Z.; Arlt, W.; Wasserscheid, P. *Fluid Phase Equilib.* **2007**, *260*, 29–35.
- (26) Prausnitz, J. M.; Lichtenthaler, R. N.; Azevedo, E. G. *Molecular thermodynamics of fluid-phase equilibria*, 2nd ed.; Prentice-Hall Inc.: Englewood Cliffs, NJ, 1986.
- (27) Renon, H.; Prausnitz, J. M. *AIChE J.* **1968**, *14*, 135–144.